DEPARTMENT OF MINERALS AND ENERGY

BUREAU OF MINERAL RESOURCES, GEOLOGY AND GEOPHYSICS

RECORD 1975/40

SIMULATION OF CARBONATE DIAGENETIC PROCESSES: FORMATION OF DOLOMITE, HUNTITE AND MONOHYDROCALCITE BY THE REACTIONS BETWEEN NESQUEHONITE AND BRINE

by

PETER J. DAVIES, B. BUBELA, AND J. FERGUSON

SIMULATION OF CARBONATE DIAGENETIC PROCESSES: FORMATION OF DOLOMITE, HUNTITE AND MONOHYDROCALCITE BY THE REACTIONS BETWEEN NESQUEHONITE AND BRINE

PETER J. DAVIES[1], B. BUBELA[2], AND J. FERGUSON[1]

1. Bureau of Mineral Resources, P.O. Box 378, Canberra City, A.C.T.
2. Baas Becking Geobiological Laboratory, P.O. Box 378, Canberra City, A.C.T.

ABSTRACT

A tank system containing sediments and brine chosen to simulate an evaporative shallow-water organic-rich sedimentary basin was allowed to evolve for 10 months. Early diagenetic reactions between nesquehonite and brine resulted in a marked increase in alkalinity. The first major change was the precipitation of monohydrocalcite spherules which formed a crust between supernatant liquid and sediment. Cores of the nesquehonite layer showed dissolution of the nesquehonite and the formation of huntite and protohydromagnesite, followed by the formation of magnesium-rich dolomite, and then dolomite of stoichiometric proportions. Calcite precipitated with dolomite within the nesquehonite layer. A second crust, precipitated within a layer of decaying filamentous algae, between the nesquehonite and calcite layers was composed of calcite, dolomite and halite.

Precipitation within the nesquehonite layer was controlled by reactions between brine and nesquehonite, leading to dissolution of nesquehonite and hydrolysis of carbonate. The formation of huntite and dolomite appears to have been aided by a high CO_3^{2-} concentration in solution, which was effected by the high salinity, and maintained by the continued dissociation of nesquehonite.

INTRODUCTION

Bubela and Ferguson (1973) described a fibreglass tank of about 4 m^3 capacity (Fig. 1A, B) which facilitated the investigation under monitored conditions of some chemical, mineralogical and biological processes which take place in sediments. The tank serves to bridge the gap between natural and laboratory (bench) systems. It allows careful coring and monitoring of conditions, with virtually "in situ" chemical analysis of the system, thus safeguarding against changes which may occur in samples from field occurrences.

As part of a program to apply experimental sedimentary systems to problems of the genesis of sedimentary Pb-Zn deposits, we used the apparatus to simulate an aerobic, highly saline shallow-water carbonate environment. As many major Pb-Zn deposits are within dolomitized limestone sequences, we hoped that the experiments would shed some light on the process of dolomitization, as well as indicating the possible extent of its influence on the mechanism of base metal complexing and precipitation. In addition, it was hoped to assess the importance of biological processes on the complexing and precipitation of base metals in a carbonate environment. Ferguson et al. (1975) and Bubela et al. (1975) discussed the fixation of base metals and the role of biological degradation in these processes. The present contribution is a report on the major diagenetic changes which occurred in the brine and the various sediments within the system. The mineral phases formed are described in detail and information is presented on the chemical variables associated with mineralogical changes. The wide-ranging investigation of the variety of sedimentary processes which were investigated placed constraints on the number and type of quantitative measurements which could be carried out. However, the results help to define the chemical interactions occurring within the supernatant brine, and in the pore waters leading to diagenetic alteration and precipitation of various carbonate species. It is considered that they have important geological significance.

METHODS

The simulated sedimentary system is shown in Fig. 1A and B.

Layer A in Fig. 1B is the supernatant brine (25% solids) which was initially collected from Port Alma, Queensland (= Port Alma brine).

Layer B is nesquehonite ($Mg\ CO_3\ 3H_2O$), which it was hoped would provide a source of $Mg^{2+} + CO_3^{2-}$ for diagenetic reactions within the system.

Layer C is crushed calcite about 10 cm thick. The calcite layer lies on a planar surface of crushed dolomite, which was included within the experiment to see if metal complexes were preferentially sited within it. In addition, a thriving algal population (Chlorococcus sp.) and coccoidal and bacillus type organisms became established within the supernatant liquid. Part of this population sedimented onto the top of the nesquehonite layer. Decaying filamentous algae were placed between the nesquehonite and calcite layers, because it was thought that these might form the locus of precipitated base metals. Temperatures fluctuated between 10 and 28°C over the course of the experiment.

The experiment lasted for 10 months, during which losses of water by evaporation were compensated for by periodic additions of the Port Alma brine. The sediments were cored on four occasions by the methods described by Bubela and Ferguson (1973), which then give minimum disturbance. Pore water was monitored for changes in pH, Eh, free H_2S, and O_2, by direct insertion of electrodes into the sediments through one-way valves in the tank. Chemical changes within the supernatant liquid were followed by atomic absorbtion spectroscopy, gas-liquid chromatography and chemical methods. The cores were analysed by X-ray radiography, x-ray diffraction and S.E.M. with attached EDAX system. Details of methodology are given in Bubela et al. (1975).

Data concerning the periodicity of sampling are given in Table 1. The most comprehensive data refer to pH, Eh and the concentration of organic carbon. Cores were taken on four occasions, two in the early part of the experiment.

RESULTS

Chemical and mineralogical changes within the system are summarized below.

Supernatant liquid

Data summarizing the major trends observed during the experiments are shown in Tables 2 and 3. The Port Alma brine was analysed before it was put in the tank, and a sample from a 200-litre storage drum was analysed after the experiment; the analyses showed no differences. The chemical changes in the brine may be summarized as follows:

a) Evaporative increase in salinity. The closeness of experimentally determined concentration factors (Table 2) to that calculated from volume changes suggests only limited mixing of supernatant and sediment pore waters.

b) The pH of the supernatant liquid rose from 6.95 to 8.1 over 3 months, and thereafter fell to 7.7 after 7.5 months (Fig. 2A). Most of the initial rise in pH occurred in the first 10 days (Table 3).

c) The alkalinity of the supernatant liquid increased from 150 ppm (for Port Alma brine) to 1500-1600 ppm. It is likely that most of this alkalinity increase accompanied the pH rise in the first 10 days. However the analyses in Table 2 indicate a high level of alkalinity by the end of 3 months.

d) The concentration of calcium decreased over the period of the experiment from 900 to 320 ppm, in spite of the fact that the concentration expected from evaporation should have been 1050 ppm. Magnesium concentration in the final supernatant liquid was marginally higher than that calculated for evaporation increases. The salinity and calcium variations caused a change in the Mg/Ca ratio from 18.4 to 63 during the experiment.

Changes similar to b, c and d could be induced experimentally in samples of Port Alma brine by shaking with excess solid nesquehonite, a calcium precipitate forming, leading to a depletion in the calcium concentration.

e) A vigorous population of green (Chlorococcus) algae and a variety of coccoidal and bacillus type organisms became established in the supernatant within 3 months. The organic carbon content of the supernatant liquid increased constantly over this period (Table 3). Some of the organic material sedimented onto the top surface of layer B (nesquehonite).

f) The particulate fraction of the supernatant liquid (brine) changed during the experiment. At the beginning, the centrifuged (10^2-10^5 x G) particulate matter was composed of mucillage and lepido-crosite. A sample centrifuged after 7.5 months showed aragonite, high-Mg calcite, unidentified Ca-Mg-carbonates, halite and mucillage. Chemical and X-ray diffraction data of this material are shown in Table 4 and Figure 3. The morphology of the aragonite shown in Figure 4B is here named "lemons". No aragonite was detected in or on the surface nesquehonite layers.

g) The supernatant brine remained oxidizing throughout the experiment.

"Crust" Precipitates

During the experiment two carbonate crusts precipitated:

a) At the junction of the supernatant and nesquehonite layers (Crust 1);

b) Within the organic layer between the nesquehonite and calcite layers (Crust 2).

Crust 1

During the first five months, a crust 3 mm thick formed at the junction of the nesquehonite and supernatant brine. This is shown in Figure 5A, B. This crust was sampled after 5 months and after 7.5 months. Cross-sectional and plan views of the crust are shown in Figure 4A, 5A, B: the outer surface is irregular and the under surface is generally smooth. The cross-sectional view shows an upper zone of spherulitic, oolitic-like bodies (Fig. 4A) approximately 0.1 mm in diameter, and a darker finer-grained portion beneath. The crust was physically disaggregated and "panned" in acetone into 3 fractions: a) sphere; b) matrix

1 - brown and fine-grained; and c) matrix 2 - light-coloured and fine-grained. X-ray analysis of the different fractions are shown in Figure 6.

The spheres fraction was totally monohydrocalcite (Fig. 6A)and chemical analysis showed that very little magnesium occurred in this fraction. Optical examination of the crust showed that the monohydrocalcite spheres were approximately 0.1 mm in diameter, of relatively uniform size, and many had an organic fragment as a nucleus (Fig. 4C). A concentric structure was visible in most (Fig. 4C), while all showed a uniaxial extinction cross (Fig. 4A, C, D, E), and a radial orientation corresponding to the slow ray direction.

Optical examination of the fine-grained lower part of the crust showed a division into two types of material, minute crystals approximately 1-2μ in size (Fig. 4C), and spherical bodies up to 20μ in diameter, some of which appear to be zoned. Also, within the fine-grained material were scattered spheriodal bodies identical to the monohydrocalcite bodies of the upper part of the crust. The scattered bodies show various stages of corrosion (Fig. 4D, E), and therefore appear to have been partly dissolved within the lower part of the crust.

SEM photographs show monohydrocalcite spheres, and cornflake-like aggregates of protohydromagnesite (Fig. 5C-F) similar to those figured in Davies & Bubela (1973). The aggregates (Fig. 5C, D, & F) are likely to be the 20μ spheroidal zoned objects seen in thin section. Also in the SEM picture are abundant egg-shaped objects approximately 5-10μ in size (Fig. 5F). Both make up the fine-grained lower portion of the crust. Huntite and protohydromagnesite were identified by X-ray within this fraction (Fig. 6B-C). Scanning electron microscope and Edax examination of the hydromagnesite and huntite fractions are shown in Fig. 7. The cornflake-like hydromagnesite and egg-shaped unidentified bodies are shown in Fig. 7A, and the X-ray image showing calcium distributions is shown in Fig. 7B. The correspondence of calcium with the egg-shaped bodies, and the occurrence of calcium in only one mineral phase identify the egg-shaped bodies as huntite.

Crust 2

Crust 2 formed within the decaying filamentous organic material between the calcite and nesquehonite layers (Fig. 8A, B, C). It was first noticed after 5 months, but was not sampled until the end of the experiment. Most of the crystals forming the crust show skeletal crystal development, with voids running through the middle of the crystals (Fig. 8C). Figure 8D shows the different nature of the crushed calcite forming layer C, below the crust. The crust X-rayed as calcite, dolomite and halite (Fig. 9). Undoubtedly some of the cubic forms in Figure 8B, C are halite. To determine the position of the dolomite, the crust was examined by electron probe (Fig. 10A, B). Figure 10A shows hexagonal crystals approximately 6 nm in size and exhibiting skeletal growth. Figure 10B shows the electron diffraction picture for magnesium. The association of magnesium and crystals with skeletal growth is apparent. A qualitative estimate of the Mg:Ca ratio from integrated counts suggests a 1:1 composition. This agrees with the X-ray data, and identifies the skeletal hexagonal crystals as dolomite of ideal composition. The 211 peak is very sharp but the ordering reflections are weak.

Nesquehonite Layer

X-ray analysis of cores of the nesquehonite layer are shown in Figure 11. The first core (Fig. 11B) showed that nesquehonite was still abundant although new peaks have appeared. The peaks were tentatively identified as protohydromagnesite (Davies & Bubela, 1973) or hydromagnesite. The 5.7Å peak may be the 111 hydromagnesite reflection. However, the 2.86Å peak is larger than the 5.7Å peak which should be the more intense. This suggests that protohydromagnesite is present, either to the exclusion of, or in addition to, hydromagnesite. The "cornflake"-like structure of the protohydromagnesite is identical to that at the top of the nesquehonite layer (Fig. 5F). A second core taken 10 days later showed a similar stage of development, but many of the nesquehonite peaks were missing (Fig. 11C).

A third core taken after the system had been functioning for 95 days showed two major developments (Fig. 11D). Firstly, all the nesquehonite peaks had become less intense and some had disappeared, e.g. 3.59 , 2.98 , 2.62 , 2.34 , 2.02Å. Secondly, magnesium-rich dolomite with a composition $Ca_{0.43}Mg_{0.57}CO_3$ is clearly visible on the diffractogram. This can only have grown diagenetically within the decomposing nesquehonite layer. There may also be calcite present. A fourth core taken after 132 days shows two features (Fig. 11E): the major carbonate phase is low-Mg calcite; the dolomite is still present, and shows a single strong peak at 2.89 (211) indicating a stoichiometric composition of $Ca_{0.5}Mg_{0.5}(CO_3)$. A fifth sample of layer B was collected immediately before the end of the experiment. This X-rayed as nesquehonite and low-Mg calcite. Kazakov et al. (1959) showed a similar terminal phase, and concluded that the paragenesis of calcite and nesquehonite were very similar.

Chemical changes within the nesquehonite layer include a large rise in pH in the first 10 days, this remaining as a plateau for 140 days, followed by a fall during the rest of the experiment down to pH6.6 (Fig. 2B). The layer remained oxidizing throughout and showed its largest increase in organic carbon in the first 100-150 days (Fig. 12A, B).

Calcite Layer (Layer C)

Four cores and a terminal sample were collected. Very little mineralogical change was evidenced on X.R.D. The only additional peaks in all the diffractograms were halite peaks.

The pH curve shows a rise due to equilibration of the calcite and brine, followed by a continuous fall for the next 150 days down to pH 7.0 after which pH gradually rose to 8.2 (Fig. 2C). For the first 100 days H_2S production increased concomitant with a marked decline in oxygen; organic carbon also increased (Fig. 12A, B).

Dolomite Layer (Layer D)

Although the dolomite layer (D in Fig. 1B) became thixotropic after two months, detectable mineralogic changes were found only in samples collected after 146 days (Fig. 13A, B).

DISCUSSION

The cause of the rise in alkalinity of the supernatant brine is attributed to the dissociation of the nesquehonite with which it is in contact. A similar increase (~20 meq/l) in alkalinity can be induced in Port Alma brine by shaking it with excess nesquehonite, the alkalinity increase occurring in 10-16 days (Ferguson et al., 1975). The nesquehonite layer shows a drop in pH after 140 days (Fig. 2B), indicating precipitation as a dominant process. This serves as a date after which little excess alkalinity was added to the supernatant liquid. The alkalinity increase in the supernatant liquid therefore occurred before 140 days. The principal effect of the alkalinity increase is the precipitation of the monohydrocalcite crust. Throughout the experiment, 616 ppm calcium was lost from solution. Most of this probably formed monohydrocalcite, which would require 31 meq/l of HCO_3^-, suggesting that further dissolution of nesquehonite occurred. It also dates the monohydrocalcite as having formed during the first 140 days, while aragonite was detected only in the later part of the experiment, and then only in the brine. The question remains as to why monohydrocalcite should precipitate before aragonite, a result duplicated during bench experiments. Previous workers have also noted this, but stressed that monohydrocalcite occurred only as an accessory to aragonite (Monaghan and Lytle, 1956; Simkiss, 1964). Lippman (1973) suggested that the Mg^{2+} ion inhibits the formation of calcite, preferentially allowing monohydrocalcite and aragonite to precipitate, a minimum molar concentration of 0.01 M Mg^{2+} being required. In the tank experiment, therefore, conditions favour the precipitation of monohydrocalcite and aragonite. The preponderance of monohydrocalcite may be due to nucleation factors and/or inhibiting factors. In previous bench experiments, precipitation of aragonite was delayed for long periods, after which sudden precipitation occurred. This is a common supersaturation phenomenon and suggests that spontaneous nucleation of aragonite is delayed. Our bench experiments also indicate that humic acids delay the onset of any precipitation and that when it does occur the first precipitate is monohydrocalcite, followed by aragonite. Furthermore, the monohydrocalcite is stained deeply brown by included organic material, while the aragonite is only

lightly stained or colourless. The organic material may therefore accentuate the previously recorded delay in the spontaneous nucleation of aragonite. The Mg^{2+} effectively stops the precipitation of calcite by "poisoning" likely calcium sites. Thus, a state of supersaturation with non-precipitation is achieved, during which the most easily precipitated salt will crystallize. Under conditions of reasonably high calcium concentration, high HCO_3^-, and pH 8, monohydrocalcite will precipitate. This is aided by the fact that total dehydration of each calcium ion is not necessary. In our tank experiment the later formation of aragonite "lemons" may be the result of lower calcium concentration and the inhibition of precipitation. Aragonite precipitation probably occurred in the period after 140 days, as suggested by the fall in pH of the supernatant.

The pH curve for both supernatant and the nesquehonite layer shows three sections. These are best illustrated by the nesquehonite curve (Fig. 2B).

AB - dissociation period

BC - supersaturation period

CD - crystallization period.

During the dissociation period, nesquehonite dissolves in contact with the brine. This may be generally written as

$$MgCo_3.3H_2O + H_2O \rightarrow Mg^{2+} + HCO_3^- + OH^-$$

It is likely, however, that two intermediate stages occur within this reaction which may be written generally as

a) $MgCO_3.3H_2O + H_2O \rightarrow Mg^{2+} + CO_3^{2-} + H^+$ - fall in pH

b) $CO_3^{=} + H^+ + H_2O \rightarrow HCO_3^- + OH^-$ - rise in pH.

If the second part (b) were completed quickly, then it would be possible to form hydromagnesite or protohydromagnesite via $4Mg^{2+} + 5CO_3^{2-} \rightarrow Mg_4(CO_3)_3(OH)_2 3H_2O + 2HCO_3^-$.

Two factors affect events in the supersaturation stage: 1. The precipitation of monohydrocalcite, which would result in further dissociation of nesquehonite; 2. The slow transformation of nesquehonite into hydromagnesite, which suggests that hydrolysis of carbonate to bicarbonate and hydroxyl was

occurring only with difficulty. Sufficient hydrolysis seems to have occurred to induce a slow pH rise (after the initial dissociation), but on occasions the production of H^+ as a preceding step may have been faster (pH drop between 20 and 55 days). The high salinity, by virtue of the effect of ionic strength on the dissociation constants, will likely induce a higher overall concentration of CO_3^{2-} in solution (Horne, 1969). During the supersaturation stage, therefore, conditions of high Mg^{2+} concentration, low calcium concentration and relatively high CO_3^{2-} concentration occur together with conditions under which OH^- is being produced with difficulty, resulting in the precipitation of huntite and dolomite. If hydroxyl had been available, hydromagnesite should have formed. The time relations between the precipitation of dolomite and huntite are not known, but the presence of huntite within the monohydrocalcite crust suggests that it formed early, perhaps by reactions between the early-formed monohydrocalcite crystals and the pore solutions in the top of the nesquehonite layer. Evidence suggesting dissolution of monohydrocalcite has already been shown (Fig. 4D, E). However the precipitation of both huntite and dolomite is significant. Kinsman (1967) suggeste that huntite is a precursor mineral to dolomite, and Lippman (1973) indicated that huntite will grow before dolomite because its more open crystalline structure will make magnesium dehydration somewhat easier. If Lippman's (op. cit.) contentio that high concentration of CO_3^{2-} is important in the dehydration of the Mg^{2+} ion, then maintaining such concentration over an extended period becomes critical to the formation of dolomite. The importance of the supersaturation stage is therefor the length of time over which it occurs (5 months). This is especially so, in view of the conclusions of Illing et al. (1965) that the difficulties of precipitating dolomite are compounded by the slowness of the reaction. This is borne out in our experiments by the appearance of dolomite in the later part of the supersaturation stage. The maintenance of high CO_3^{2-} concentration throughout this stage, by the slow decomposition of nesquehonite, may therefore be critical to the dolomite formation.

Our experimental results closely parallel Lippman's hypothesis that if alkalinity production is rapid, then hydrous magnesium carbonates may precipitate

as precursors to dolomite (see also Kinsman, 1967). These may in turn react with solutions, providing a reservoir of Mg^{2+} and Ca^{2+} for the formation of dolomite. Similarly, the double carbonate huntite should be expected to form a precursor to dolomite formation (Lippman, 1973, p.188).

The length of the supersaturation stage in our experiments is much longer than previously reported (Kazakov et al., 1959). In addition, other major differences in our experiments are high salinity and high organic material. The high salinity serves to increase the solubility of nesquehonite, and the organic material delays the precipitation of carbonate phases (Kazakov et al., 1959; Chave, 1970). Both factors contribute to maintaining a suitable environment over a sufficiently long period for the formation of dolomite.

Despite the almost universal acceptance that the Mg^{2+}/Ca^{2+} ratio is critical in the formation of dolomite (Von der Borch, 1965; Deffeyes et al., 1965; Kinsman, 1965; Liebermann, 1967; Glover and Sippel, 1967; Bathurst, 1971), some experimental work indicates that this is not necessarily so (Siegel, 1961; Fritz and Smith, 1970; Erenberg, 1961; Müller and Fishbeck, 1973; Chazen and Ehrlick, 1973). Sonnenfeld (1963) suggested that the concentration of anions was more important than the concentration of cations, and Bentor (1961) pointed out that in many places a high Mg^{2+}/Ca^{2+} ratio bore no relation to dolomitization. Lippman (1973) concluded that the Mg^{2+}/Ca^{2+} ratio only became important after sufficient CO_3^{2-} was available. In our own experiments the Mg^{2+}/Ca^{2+} ratio in the brine varied between 18.4 and 63. We cannot comment about the ratio in the nesquehonite layer, especially if some dissolution of monohydrocalcite was occurring as indicated by thin section examination.

There were no mineralogic changes, recognized by X-ray diffraction, within the calcite layer. However, the pH curve (Fig. 2C) indicates that changes did occur, involving only solution and reprecipitation of calcite. The pH curve shows an initial rise due to equilibration of calcite and brine; this is the dissociation stage. The ensuing supersaturation stage is short (10-14 days), and is followed by a precipitation stage (fall in pH). The duration of the

supersaturation stage is only fractionally longer than the time required for the precipitation of calcite in laboratory experiments (200 hours - J. James, personal communication, 1975). The precipitation stage requires an influx of CO_2 to accommodate H^+ released from the dissociation of HCO_3^- to CO_3^{2-}. The CO^2 may have originated in the nesquehonite or the dolomite layer. However, the dolomite layer was requiring CO_2 to accommodate its own precipitation-induced fall in pH, and CO_2 may have been released slowly from the nesquehonite layer during its supersaturation stage. A further possibility is the oxidative decomposition of organic material between the nesquehonite and calcite layers, and also the organic material within the calcite layer. The Eh curve for the calcite layer (Fig. 12) shows a drop during the precipitation stage, indicating consumption of oxygen. At the same time organic carbon increases, suggesting that additional organic material was being cycled to restore any lost through oxidation. The most abundant source of organic material was the layer of decaying filamentous algae between the calcite and nesquehonite layers. This layer should therefore provide a site near which precipitation should occur most readily because of the ready access of CO_2. It is in this position that the second crust was precipitated. The time of formation of the crust cannot be pinpointed, but the occurrence of dolomite within the crust is important. The dolomite seemingly occurs as a precipitate. Its position within organic material may be crucial. The source of Mg^{2+} is undoubtedly the brine while the source of alkalinity is that induced by calcite and nesquehonite dissociation. The pH of the calcite precipitation stage extends from 8.2 to 7.1, only a small part of which (0.1 pH unit) compares with the period of dolomite formation in the nesquehonite layer. This suggests that the "organic dolomite" either precipitated very early, or formed under very different pH conditions. Extending our conclusion that dolomite precipitates very slowly, it is unlikely that the organic dolomite would have precipitated early during the 2-3 days when the pH was similar to that in the nesquehonite supersaturation stage. It is more likely that the dolomite precipitated during the time of falling pH within the calcite layer, and as such must therefore be different from the dolomite which formed in the nesquehonite layer, all of which dissolved during the precipitationally -induced pH drop.

The inverse relations between the pH curves for the calcite and nesquehonite layers (Fig. 14) suggests a genetic relation, especially in the period 140 to 300 days. It is likely, therefore, that the CO_2 increase accompanying the pH drop in the nesquehonite layer was due to a slow leakage of CO_2 from the calcite layer. This would have been largely trapped in the nesquehonite layer by the crust of monohydrocalcite. That this was not an effective trap is indicated by the drop in pH of the supernatant layer after 140 days. However, the slight terminal rise in the supernatant pH indicates that losses were greater than gains towards the end of the experiment.

In the dolomite layer, the magnitude of the pH changes in the first 100 days is less than in the other layers. Some dissolution of dolomite probably occurred early, but this cannot be shown by X-ray data. However, X-ray data show precipitation of calcite within this layer before 146 days, when the pH was approximately 7.2-7.3. In other words, calcitization of the dolomite layer has occurred.

GEOLOGICAL RELEVANCE

In our experiments we have not tried to simulate any particular natural environment because insufficient is known about such environments. The experiments were carried out under conditions which approximate to an aerobic shallow-water evaporitic basin (Table 5). Its similarities to chemical and physical conditions in the Coorong of South Australia have been indicated by Ferguson et al. (1975). Although large quantities of nesquehonite have not been reported in modern evaporitic environments, its use is justified on various grounds. Firstly, it was used primarily as a source of alkalinity and not as a source of magnesium. We did not use hydromagnesite because we did not want the pH to rise much above 8 (see Glover and Sippel, 1967). The subsurface pH in the Persian Gulf dolomitic province fluctuates between 6 and 7 (Illing et al., 1965; Kinsman, 1967), and Liebermann (1967) showed experimentally that dolomitic carbonates precipitate around pH 8.1. Secondly, previous work (Davies and Bubela, 1973) showed that nesquehonite altered relatively slowly to hydromagnesite via an

unstable intermediate phase, protohydromagnesite. Thirdly, our own work and that of Kazakov et al. (1959) indicate that the paragenesis of nesquehonite is similar to that of calcite. The incorporation of magnesium into a calcite-type lattice is most likely to produce dolomite. Evidence for this has been reported from the Coorong (Von der Borch, 1965) where dolomite and calcite underlie aragonite and hydromagnesite. Fourthly, Lippman (1973) suggested that nesquehonite or hydromagnesite may form precursors to dolomite formation; evidence for this is the precipitation of dolomite in certain Crimean lakes where bicarbonate of river water reacts with magnesium salts (Liebermann, 1967, p. 245). In addition, we recently identified nesquehonite in dolomitic lakes in the Coorong.

Although the precipitation of a mineral species depends on two parts of a solubility product, almost all workers have explained the origin of dolomite by variations in the cationic ratio Mg^{2+}/Ca^{2+}. It is noteworthy that in all areas where recent dolomites have been reported, except Bonaire, no data are given for alkalinity. Thermodynamic data suggest that seawater is supersaturated with respect to dolomite (Halla and Ritter, 1935; Garrels and Thompson, 1960; Hsu, 1969; Berner, 1971; Lippman, 1973). The cationic components are therefore present in sufficient quantities (Lippman, 1973) but the CO_3^{2-} concentration is low, and dolomite does not precipitate. Dolomite forms at Bonaire, where the alkalinity varies from slightly below to well above that of seawater. More significant, however, is that Deffeyes et al. (1965) showed that CO_3^{2-} concentration increased markedly over the HCO_3^- (Deffeyes et al., 1965, Table 1, p. 76).

No alkalinity data have been published for Coorong lakes. The data in Table 5 for Lake Fellmongery are therefore informative; the alkalinity varies from 680 ppm (February) to 564 ppm (November); this is roughly five times the concentration of seawater. Groundwater near lakes in the area has a HCO_3^{2-} concentration of about 435 ppm (Taylor, in press). The same author reported that high-Mg calcite with 33 mole % $Mg\ CO_3$ is precipitating within Lake Fellmongery, but dolomite sensu stricto is not. The Mg^{2+}/Ca^{2+} ratio varies between 10 and 20 which is within the range shown by Von der Borch (1965) for the dolomite-

precipitating lakes. The non-precipitation of dolomite at Lake Fellmongery appears to contradict our hypothesis. However, Von der Borch (op. cit.) also stipulated a pH up to 10 as a requirement in the dolomite lakes, whereas at Lake Fellmongery the pH never rises above 8.6. Thus in spite of the high alkalinities, in any alkalinity partition the concentration of HCO_3^- will greatly exceed CO_3^{2-}. According to Von der Borch's data, the Coorong is exceptional because of its high pH and relatively low salinity (see also Bathurst, 1971). In the Persian Gulf, dolomite is forming under conditions of low pH (6 to 7) and very high salinity (6 x S.S.W.). The combination of these two factors results in: a) the precipitation of calcium sulphate, which leads to an increase in the solubility of previously precipitated metastable calcium carbonate phases; b) dissolution of the calcium carbonate phases, resulting in an increase in alkalinity; and c) the high salinity ensures a high proportion of CO_3^{2-} to HCO_3^-. The formation of dolomite may therefore occur under two different chemical conditions, both of which lead to the same requirement of an increase in the CO_3^{2-} concentration.

In our experiments we have precipitated three important phases (monohodryocalcite, huntite and dolomite) under conditions of high alkalinity.

Monohydrocalcite has only previously been reported three times from recent environments (Sapozhnikov and Tsvetkov, 1959; Fishbeck and Müller, 1971; Taylor, in press). It has been synthesized in the laboratory by numerous workers, usually by the addition of organic or inorganic additives (Brooks et al., 1950; Kinsman and Holland, 1969; Malone and Towe, 1970; Duedall and Buckley, 1971). Taylor (in press) has described monohydrocalcite forming a beach rock around Lake Fellmongery. He has concluded that although monohydrocalcite was not reported in the carbonate lake sediments of the Coorong, X-ray diffraction data have consistently revealed small quantities. In addition, field studies at Lake Fellmongery show that the monohydrocalcite alters to high-Mg calcite containing 33 mole % $MgCO_3$; it therefore appears that monohydrocalcite is a precursor to a mineral approaching dolomitic composition.

It has been suggested that monohydrocalcite forms either from airborne water droplets (Marschner, 1969; Fishbeck and Müller, 1971), or is due to organic

activity (Broughton, 1972; Malone and Towe, 1970). In our work, and in that of Taylor (op. cit.), the nucleii of the monohydrocalcite spherules are organic fragments. More important, however, is the role of soluble organic material and mucus. These and high magnesium concentration ensure that aragonite is inhibited, and that calcite does not precipitate. Monohydrocalcite precipitates in the meantime. Dissolution of monohydrocalcite occurred in our tank below the top of the crust, where it is surrounded by unstable magnesium phases. It is therefore possible that this is the source of calcium for the precipitation of huntite within the crust.

Kinsman (1967) reviewed the occurrence of huntite, and described its occurrence in Recent sediments of the Trucial Coast; he postulated that huntite grows as a metastable phase occupying the stability field of dolomite. The physical conditions in our tank experiment are similar to those postulated by Kinsman (op. cit.). However, huntite was not precipitated in bench experiments inducing rapid precipitation, the metastable phases aragonite and hydromagnesite occupying the stability fields of more stable counterparts. This suggests that huntite, like dolomite, is much slower to precipitate. The higher percentage of organic material in Crust 1 (4.4% organic carbon) may therefore have aided in suppressing other carbonate phases.

In our tank experiments, dolomite formed both within the nesquehonite layer and within an organic-rich crust between the nesquehonite and calcite layers.

In the nesquehonite layer, dolomite and calcite precipitate as diagenetic phases. In the Coorong, Von der Borch (1965) described a "hydromagnesite lake" in which the surface sediments are hydromagnesite and aragonite, but in which the subsurface sediments are dolomite and calcite. If the ground-water near the "hydromagnesite lake" is similar to that around Lake Fellmongery, then the alkalinity will likely exceed 435 ppm (Taylor, in press). The pH of such groundwater is approximately 7.9. If this comes into contact with hydromagnesite and aragonite, dissolution of these phases will occur under conditions of high bicarbonate alkalinity. At the end of the wet season or early in the dry season,

marked salinity increase will result in a high CO_3^{2-} concentration which will promote dolomite and calcite precipitation.

In contrast to "dolomite-precipitating lakes", the "hydromagnesite lake" supports very little plant life (Von der Borch, op. cit., mentioned the absence of Ruppia sp.). In this lake, therefore, it is likely that the organic content of the water is low, and that quick precipitation of metastable phases may occur.

Insufficient data are available regarding the "dolomite lakes" to explain the formation of the dolomite. However, compared with our tank experiment, four features of this environment are significant: 1. the alkalinity of the groundwater is likely to be high; 2. the salinity of the lake water is generally low; 3. plants (Ruppia) are especially abundant in areas where dolomite occurs; and 4. pH is generally high. The low salinity indicates that the mechanism required for increasing CO_3^{2-} concentration is the very high, photosynthetically induced pH acting on water which is already high in bicarbonate alkalinity. The high organic activity also means a high organic content in the water, inhibiting other carbonate phases forming. Thus, apart from the salinity, the Coorong dolomite is forming in an environment similar to our tank experiment except that the high CO_3^{2-} concentration is being caused by a photosynthetic coupled pH rise.

Gebelein and Hoffman (1973) described a secondary mode of formation of dolomite in stromatolitic sequences, which depends on a selective up-take of magnesium relative to calcium by the organic material; precipitation of dolomite presumably occurs when the magnesium is released during organic decay. These authors produced a high-Mg calcite with 17-20 mole % Mg CO_3. Thus, the dolomite which formed within the organic material in our experiment may be important. Oxidation of the organic material leads to carbonate precipitation nearest the source of the oxidate. Figures 8, 9 and 10 show that dolomite has precipitated within the organic material, the position of which between the calcium and magnesium layers suggests a Mg^{2+}/Ca^{2+} ratio unlikely to be high.

ACKNOWLEDGEMENTS

We wish to thank G. Berryman and D. Barnes for the X-ray diffraction data, and I. Johns and Dr A.G. Turnbull for scanning electron microscopy and energy dispersive results. The Baas Becking Geobiological Laboratory is supported by the Bureau of Mineral Resources, the Commonwealth Scientific and Industrial Research Organization and the Australian Mineral Industries Research Association Limited. The paper is published with the permission of the Director, Bureau of Mineral Resources, Geology and Geophysics, Canberra.

REFERENCES

Bathurst, R.G.C., 1971. Carbonate sediments and their diagenesis. Elsevier, Amsterdam, London, New York,

Bentor, Y.K., 1961. Some geochemical aspects of the Dead Sea, and the question of its age. Geochim. Cosmochim. Acta., 25: 239-260.

Berner, R.A., 1971. Principles of chemical sedimentology. McGraw-Hill, New York,

Brooks, R., Clark, L.M. and Thurston, E.G., 1950. Calcium carbonate and its hydrates. Phil. Trans. Royal Soc., 243A: 145-167.

Broughton, P.C., 1972. Monohydrocalcite in speleathems: an alternative interpretation. Contr. minerol. petrol., 36: 171-174.

Bubela, B. and Ferguson, J., 1973. Apparatus for studies of artificial sediments. J. Sediment. Petrol., 43: 1167-1170.

Bubela, B., Ferguson, J. and Davies, P.J., 1975. Biological and abiological processes in a simulated sedimentary system. J. Geol. Soc. Aust. (in press).

Chave, K.E., 1970. Carbonate-organic interactions in sea water. In: D.W. Hood (Editor), Organic matter in natural waters. Ins. Mar. Sci. (Alaska), Occasional Publ. 1.

Chazen, P.D. and Ehrlick, R., 1973. Low-temperature synthesis of dolomite from aragonite. Geol. Soc. Am. Bull., 84: 3627-3634.

Davies, P.J. and Bubela, B., 1973. The transformation of nesquehonite into hydromagnesite. Chem. geol., 12: 289-300.

Deffeyes, K.S., Lucia, F.J. and Weyl, P.K., 1965. Dolomitization of Recent and Plio-Pleistocene sediments by marine evaporite waters on Bonair, Netherlands Antilles. In: L.C. Pray and R.C. Murray (Editors), Dolomitization and limestone diagenesis; a symposium - Soc. Econ. Palaeont. Mineral., Spec. Publ. 13: 71-88.

Duedall, I.W. and Buckley, D.E., 1971. Calcium carbonate monohydrate in seawater. Nature, Phys. Sci., 234: 39-40.

Erenberg, B.G., 1961. Artificial mixed carbonates in the $CaCO_3$ $MgCO_3$ series. Z. Strukt. Khim., 2: 178-182.

Ferguson, J., Bubela, B. and Davies, P.J., 1975. Simulation of sedimentary ore-forming processes: concentrations of Pb and Zn in organic and Fe-bearing carbonate sediments. Geol. Rundschau (in press).

Fishback, R. and Müller, G., 1971. Monohydrocalcite, hydromagnesite, nesquehonite, dolomite, aragonite and calcite in speleothems of the Frankishe Schweiz, Western Germany. Contr. Mineral. Petrol., 33: 87-92.

Fritz, P. and Smith, D.G.M., 1970. The isotopic composition of secondary dolomites Geochim. Cosmochim. Acta., 34: 1161-1173.

Garrels, R.M. and Thompson, M.E., 1962. A chemical model for seawater at 25°C and one atmosphere total pressure. Am. J. Sci., 260: 77-66.

Gebelein, C.D. and Hoffman, P., 1973. Algal origin of dolomite laminations in stromatolitic limestone. J. Sediment. Petrol., 43: 603-613.

Glover, E.D. and Sippel, 1967. Synthesis of magnesium calcites. Geochim. Cosmochim. Acta. 31: 603-613.

Halla, F. and Ritter, F., 1935. Eine method zur bestimmung der freien energie bei reaktionen des typus A(s) = B(s) und ihre anwehdung auf das dolomit problem. Z. Phys. Chem., 175A: 63-82.

Horne, R.A., 1969. Marine chemistry. Wiley-Interscience, New York, 568 pp.

Hsu, K.J., 1967. Chemistry of dolomite formation: In: G.V. Chillingar, (Editor), Carbonate rocks, B: 169-191. Elsevier, Amsterdam.

Illing, L.V., Wells, A.J. and Taylor, J.C.M., 1965. Penecontemporary dolomite in the Persian Gulf. In: L.C. Pray and R.C. Murray (Editors), Dolomitization and Limestone diagenesis: A symposium - Soc. Econ. Palaeont. Mineral., Spec. Publ. 13: 89-111.

Kazakov, A.V., Tikhomirova, M.M. and Plotnikova, V.I., 1959. The system of carbonate equilibria. Int. Geol. Rev., 1(10): 1-39.

Kinsman, D.J.J., 1965. Dolomitization and evaporite development, including anhydrite, in lagoonal sediments, Persian Gulf. Geol. Soc. Am., Spec. Pap., 82: 108-109 (abst.).

Kinsman, D.J.J., 1967. Huntite from a carbonate-evaporite environment. Am. Mineral., 52: 1332-1340.

Kinsman, D.J.J. and Holland, H.D., 1969. The co-precipitation of cations with $CaCO_3$ - IV. The co-precipitation of Sr^2 - with aragonite between 16^o - 96^oC. Geochim. Cosmochim. Acta, 33: 1-17.

Liebermann, O., 1967. Synthesis of dolomite. Nature, 213: 241-245.

Lippman, F., 1973. Sedimentary carbonate minerals. Springer-Verlag, Berlin, 288 pp.

Malone, G.P. and Towe, K.M., 1970. Microbial carbonate and phosphate precipitates from sea water cultures. Mar. Geol., 9: 301-309.

Marschner, H., 1969. Hydrocalcite ($Ca\ CO_3\ H_2O$) and nesquehonite ($Mg\ CO_3\ 3H_2O$) in carbonate scales. Science, 165: 1119-1121.

Monaghan, P.H. and Lytle, M.A., 1965. The origin of calcareous oolites. J. Sediment. Petrol., 26: 111-118.

Müller, G. and Fishbeck, R., 1973. Possible natural mechanism for protodolomite formation. Nature, Phys. Sci., 242: 139-141.

Sapozhnikov, D.G. and Tsvetkov, A.J., 1959. Precipitation of hydrous calcium carbonate on the bcttom of the Lake Issyk Kulz Dokl. Acad. Nauk. SSSR., 124: 131-133.

Siegel, F.R., 1961. Factors influencing the precipitation of dolomitic carbonates. State Geol. Survey Kansas Bull., 152: 127-158.

Simkiss, K., 1964. Variations in the crystalline form of calcium carbonate precipitated from artificial sea water. Nature, 201: 492-493.

Sonnenfeld, P., 1963. Dolomites and dolomitization. A review. Bull. Can. Petrol. Geol., 12: 101-132.

Taylor, G.F., 1975. Monohydrocalcite: Its occurrence and diagenesis in two small lakes in the southeast of South Australia. Am. Miner. (in press).

Von der Borch, C., 1965. The distribution and preliminary geochemistry of modern carbonate sediments of the Coorong area, South Australia. Geochim. Cosmochim. Acta, 29: 781-799.

FIG. 1. Diagrammatic (A) and photographic (B) illustrations of the simulated sedimentary system. In the photographic illustration, the supernatant layer (A), nesquehonite layer (B), crushed calcite layer (C), dolomite layer (D), sedimented unicellular algae, and decaying filamentous algae are shown.

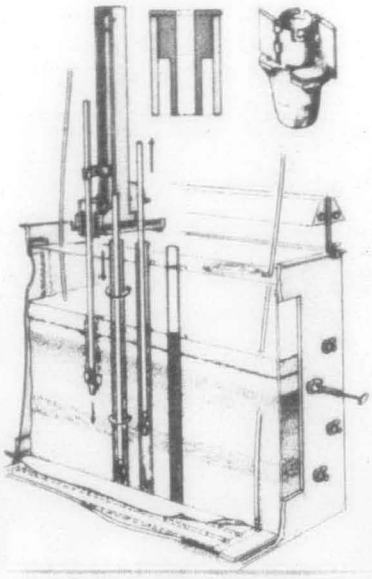

A

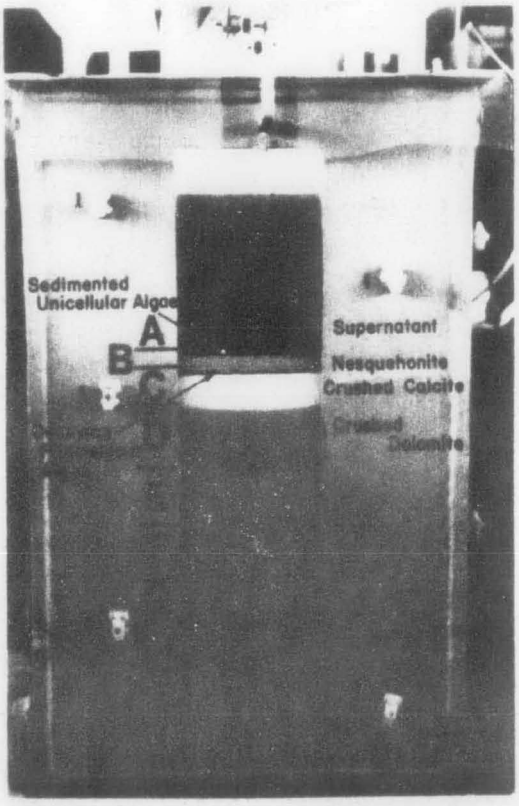
Sedimented
Unicellular Algae
A
B
C
Supernatant
Nesquehonite
Crushed Calcite
Crushed
Dolomite

B

FIG. 2 pH: Time curves for the supernatant (A), nesquehonite (B), calcite (C) and dolomite (D). C1-C4 represent cores taken at specific intervals.

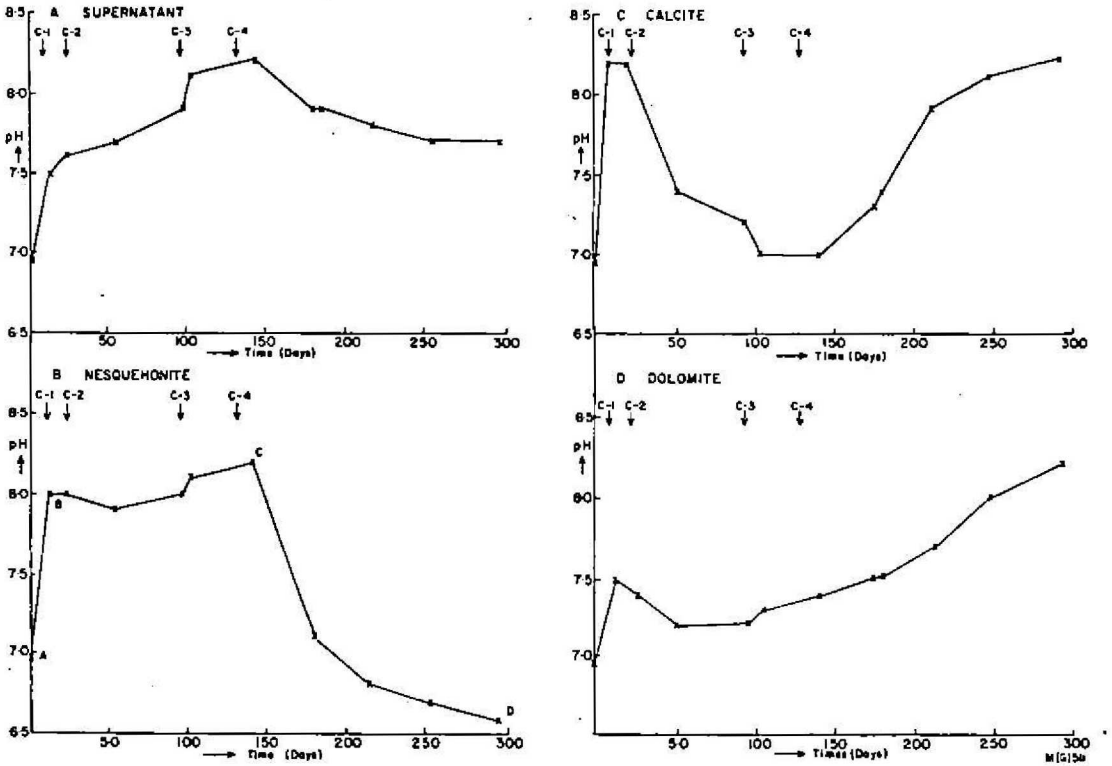
A SUPERNATANT
B NESQUEHONITE
C CALCITE
D DOLOMITE
C-1
C-2
C-3
C-4
pH
Time (Days)
8·5
8·0
7·5
7·0
6·5
50
100
150
200
250
300
A
B
C
D
M(G)5a

FIG. 3 X-ray diffraction of particulate matter fractionated from the supernatant brine 7.5 months after establishing the sedimentary system.

A1 = Separation with 100 x g
A2 = Separation with 500 x g
A3 = Separation with 3000 x g
A4 = Separation with 14000 x g

The peaks identified are aragonite (A), Halite (H), high magnesium calcites (HMC) and calcium-magnesium carbonates (Ca-Mg Carbs).

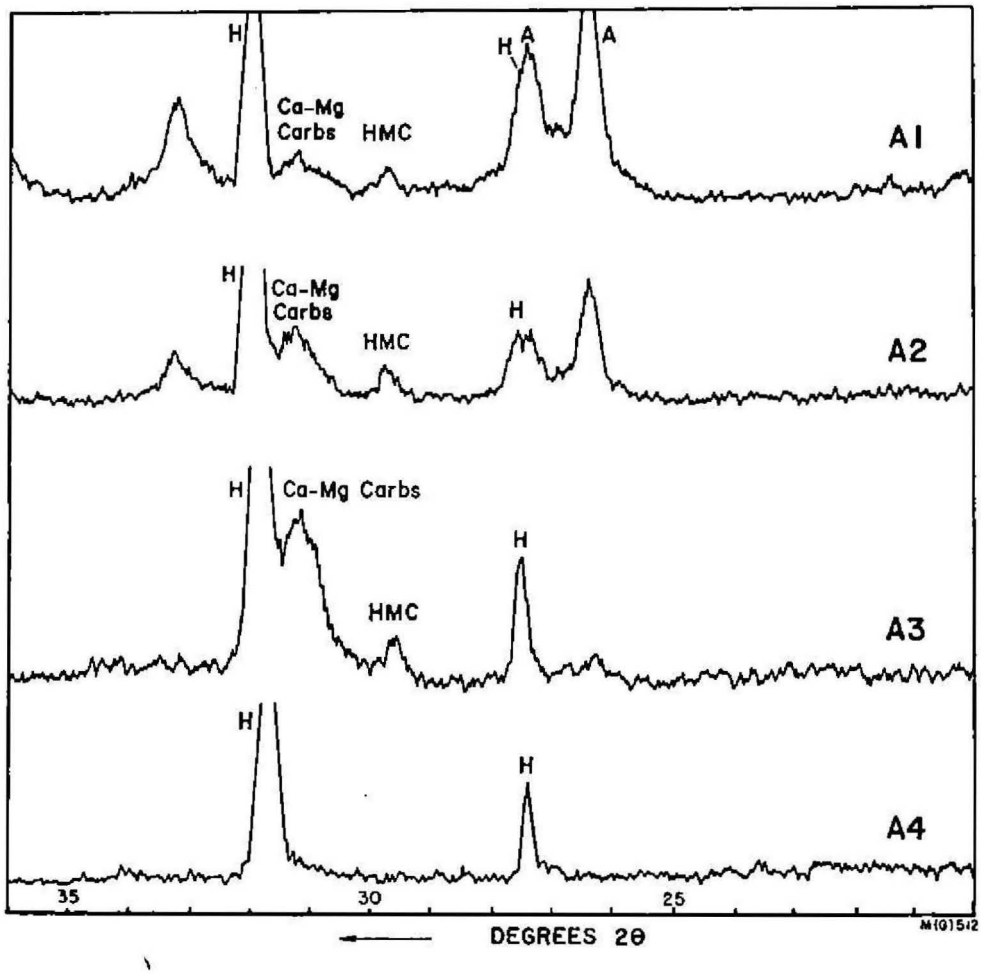
H
Ca-Mg
Carbs
HMC
H
A
A
A1
H
Ca-Mg
Carbs
HMC
H
A2
H
Ca-Mg Carbs
HMC
H
A3
H
H
A4
35
30
25
DEGREES 2θ
M(G)5/2

FIG. 4. A. Cross-section of the monohydrocalcite crust showing the spheres and fine-grained carbonate beneath. Crossed polarizers.

B. Scanning electron micrograph of aragonite "lemon" from the supernatant brine.

C. Monohydrocalcite spherule showing concentric banding and an algal fragment acting as a nucleus. Fine-grained carbonate surrounds the spherules. Plane polarized light.

D, E. Partial solution of monohydrocalcite spherules. Crossed polarizers.

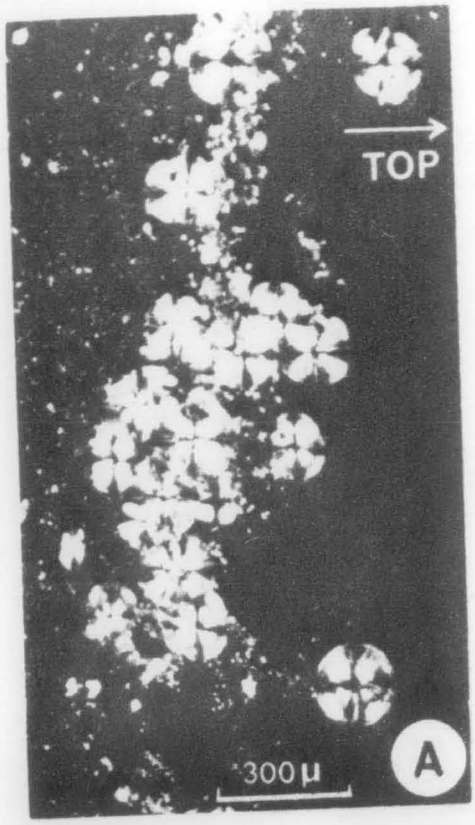
TOP
300 µ
A

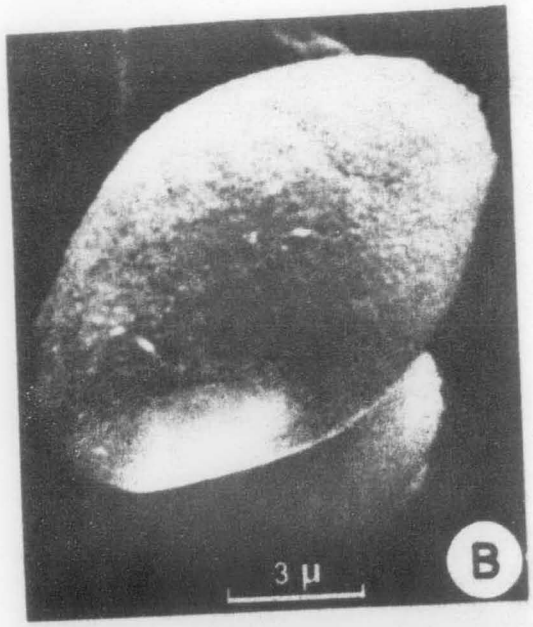
3 µ
B

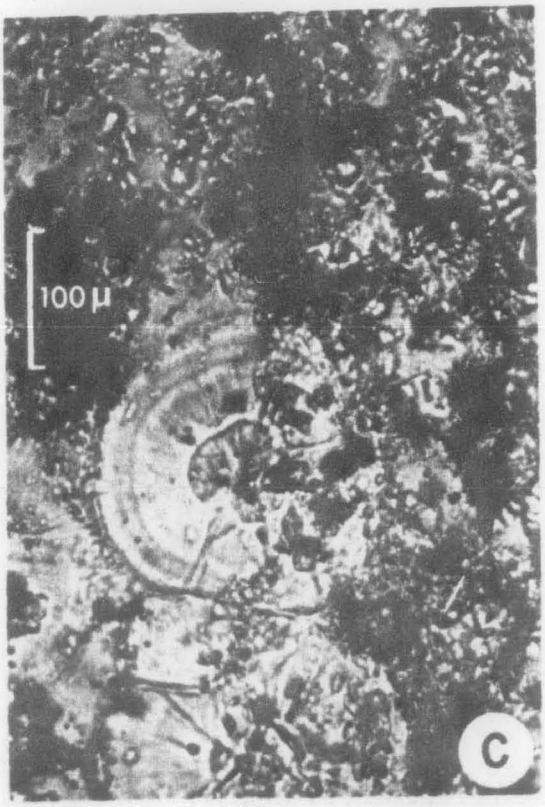
100 µ
C

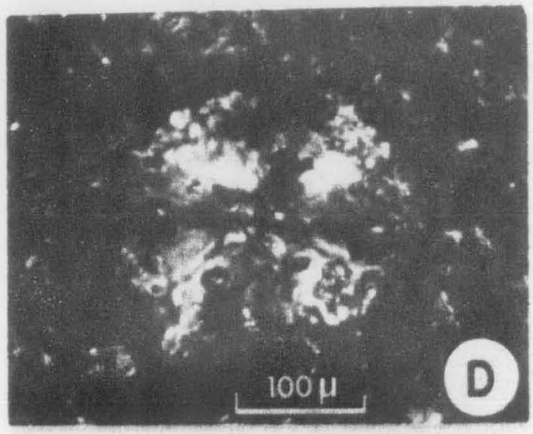
100 µ
D

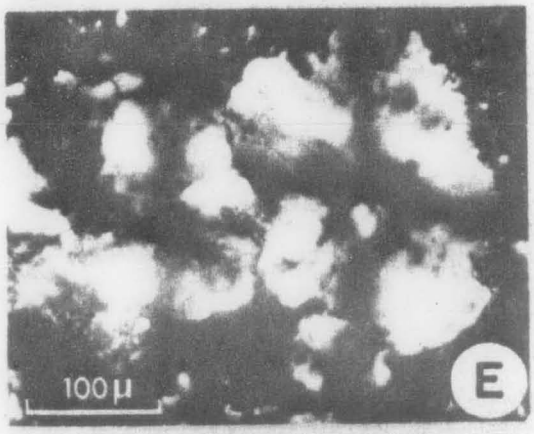
100 µ
E

FIG. 5. A, B. Plan views of the monohydrocalcite crust.

C, D. Scanning electron micrographs of the crust showing monohydrocalcite spheres, and a cornflake-like aggregate of hydromagnesite/protohydromagnesite.

E. Scanning electron micrograph of the surface of one of the monohydrocalcite spherules showing the radial orientation of crystals.

F. Scanning electron micrograph of the cornflake-like aggregate of hydro/proto-hydromagnesite and the small egg-shaped huntite crystals.

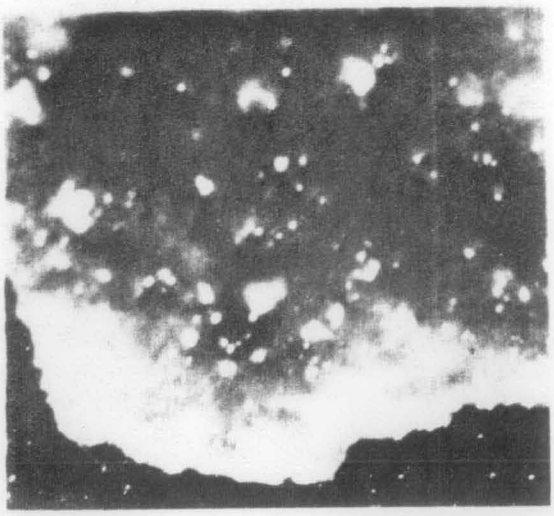

A

1 mm

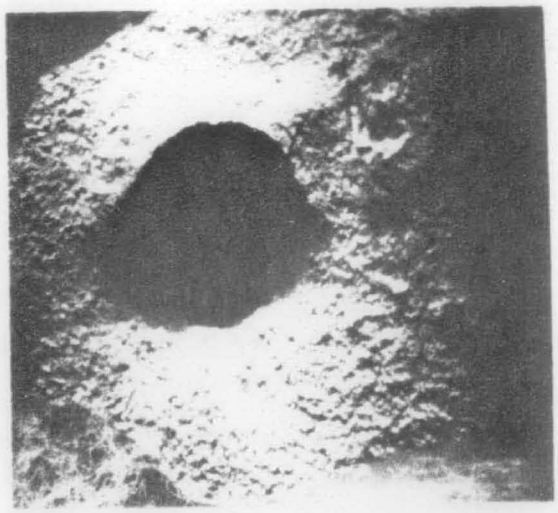

B

10 mm

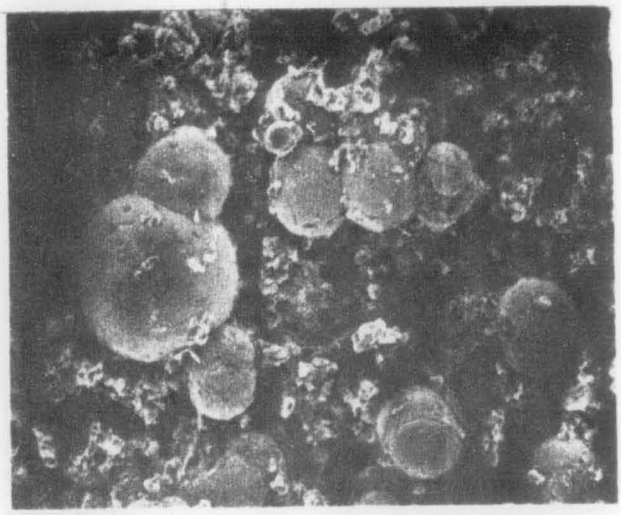

C

100 μ

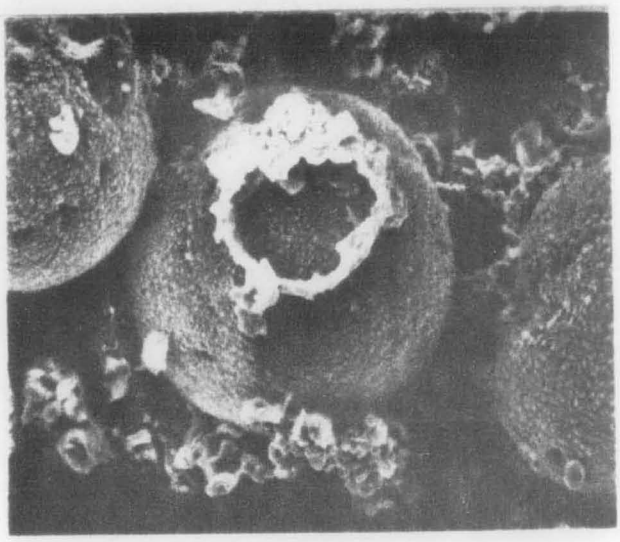

D

100 μ

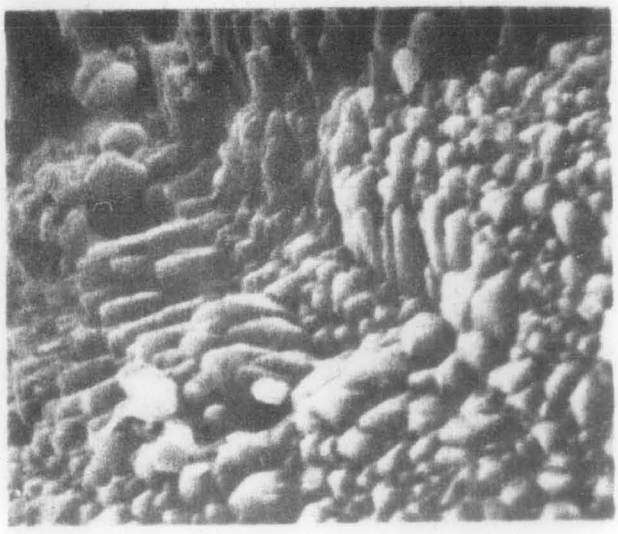

E

10 μ

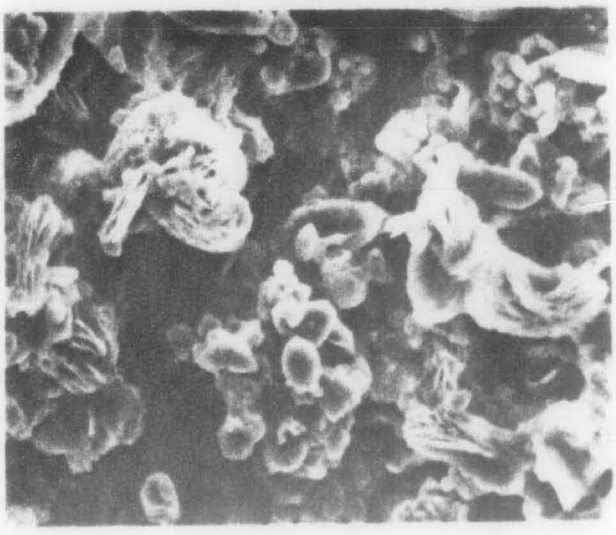

F

10 μ

FIG. 6. X-ray diffraction curves for the spheres (A), cornflakes (B), and egg-shaped portions of the crust.

M = monohydrocalcite

HU = Huntite

PROTOHYDROM = Protohydromagnesites

HYDROM = Hydromagnesites

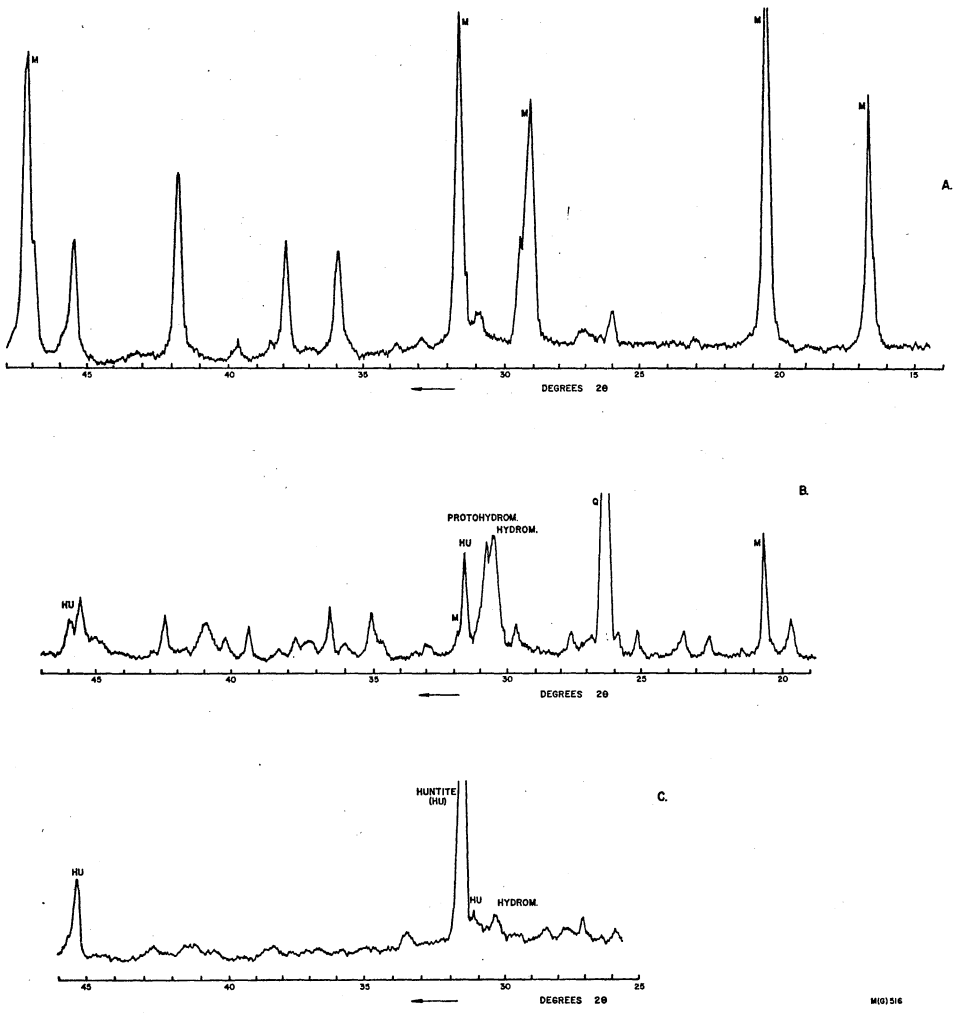
M
M
M
M
M
A.
45
40
35
30
25
20
15
DEGREES 2θ
B.
HU
PROTOHYDROM.
HYDROM.
HU
Q
M
M
45
40
35
30
25
20
DEGREES 2θ
C.
HUNTITE
(HU)
HU
HU
HYDROM.
45
40
35
30
25
DEGREES 2θ
M(G) 516

FIG. 7. A. Scanning electron micrograph of the hydromagnesite/protohydromagnesite (cornflakes) aggregates and the much smaller egg-shaped aggregates.

B. X-ray diagram showing the co-occurrence of calcium with the egg-shaped objects, confirming their identification as huntite.

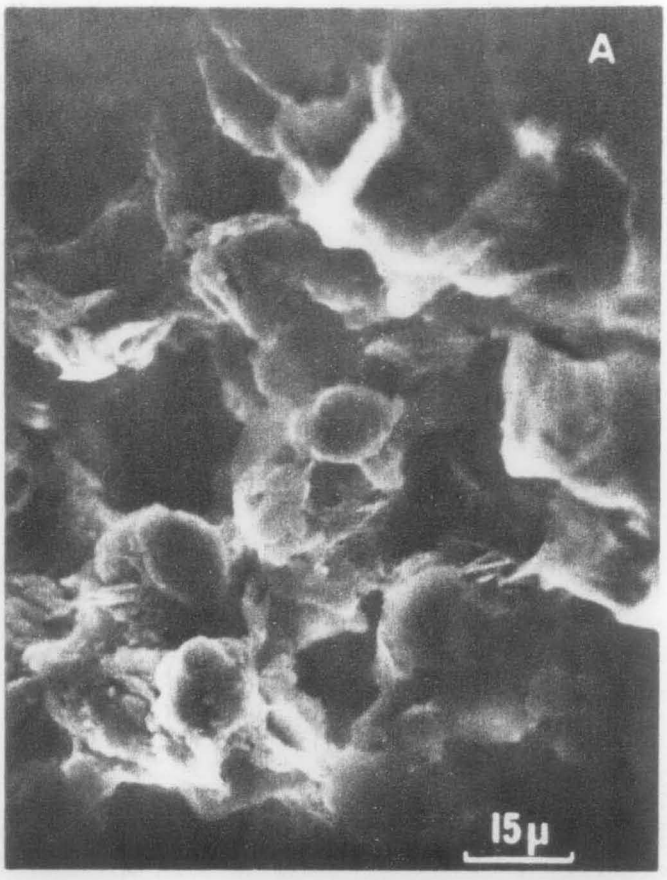
A
15μ

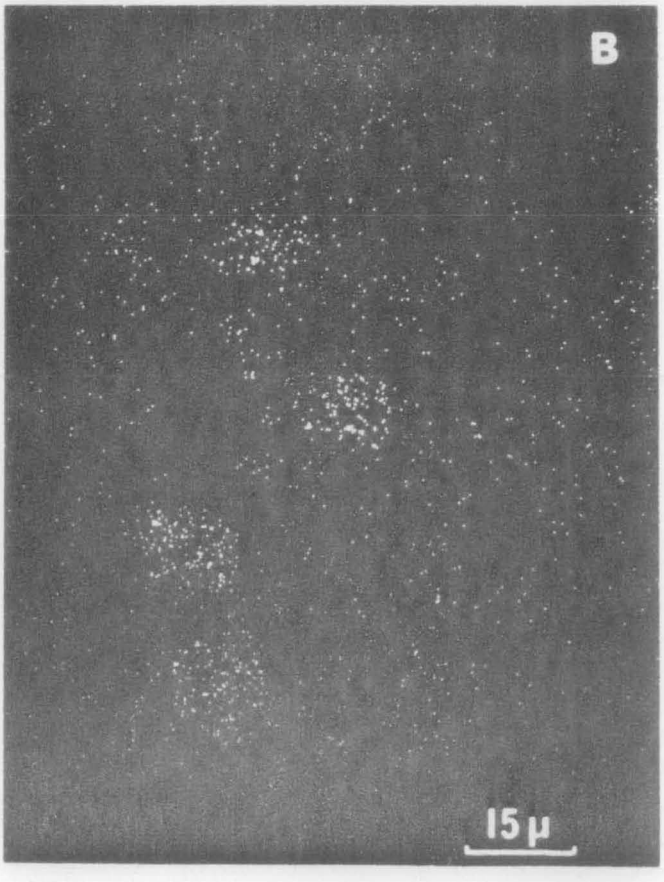
B
15μ

FIG. 8. Scanning electron micrographs of the crust which formed between the nesquehonite and calcite layers. An intimate relation of organic material and precipitated crust (8a, b) and the skeletal growth of crystals (8c) are apparent. The nature of the calcite in the calcite layer is shown in 8d.

In 8a scale bar = 500 nm

8b scale bar = 200 nm

8c scale bar = 100 nm

8d scale bar = 200 nm

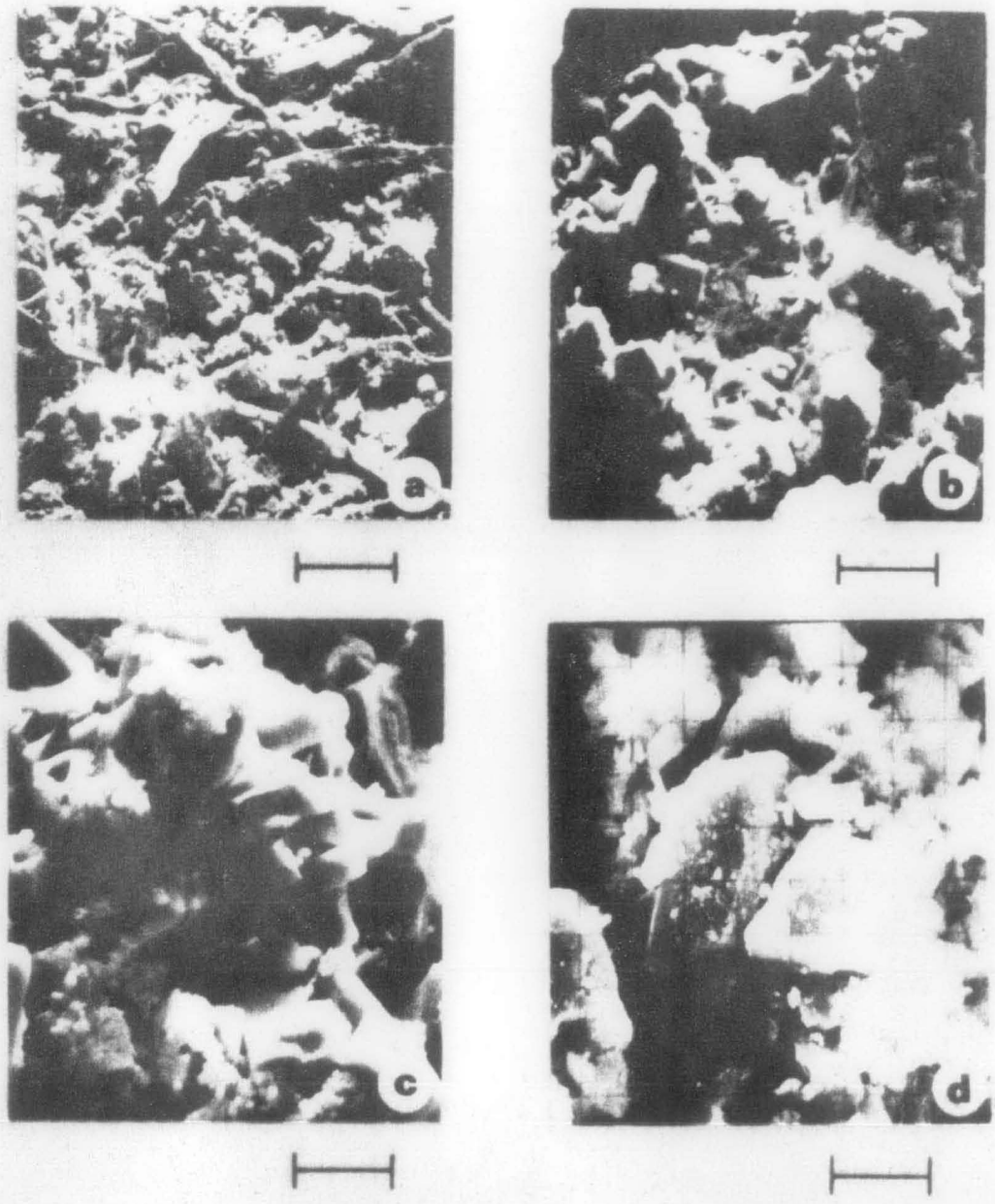
a
b
c
d

FIG. 9 X-ray diffraction of the crust between the calcite and nesquehonite layers.

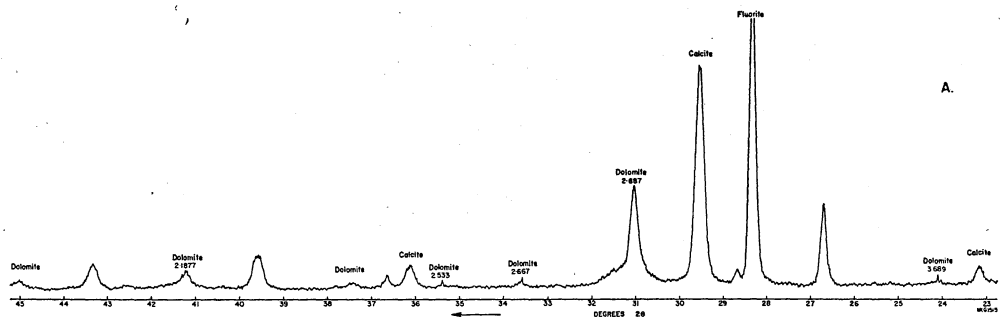
Fluorite
Calcite
A.
Dolomite 2·887
Dolomite
Dolomite 2·1877
Dolomite
Calcite
Dolomite 2·533
Dolomite 2·667
Dolomite 3·689
Calcite
45 44 43 42 41 40 39 38 37 36 35 34 33 32 31 30 29 28 27 26 25 24 23
DEGREES 2θ
MOLYBDENUM

FIG. 10 a. Scanning electron micrograph showing skeletal growth of two hexagonal shaped crystals from Crust 2.

b. X-ray distribution of magnesium. High quantities of magnesium are noticeably associated with the hexagonal crystals showing skeletal growth. These are likely to be dolomite.

Scale Bar = 3 nm.

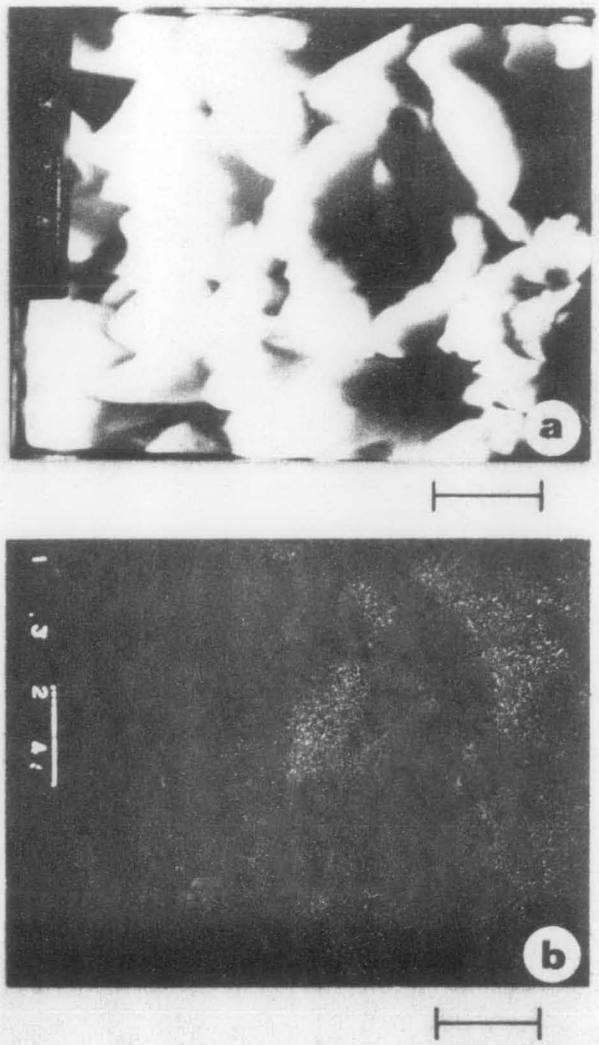
a
b

FIG 11. X-ray diffractograms of samples from the nesquehonite layer.

A = Before the experiment

B = Core after 10 days

C = Core after 23 days

D = Core after 93 days

E = Core after 130 days

N = nesquehonite; C = calcite, D = dolomite

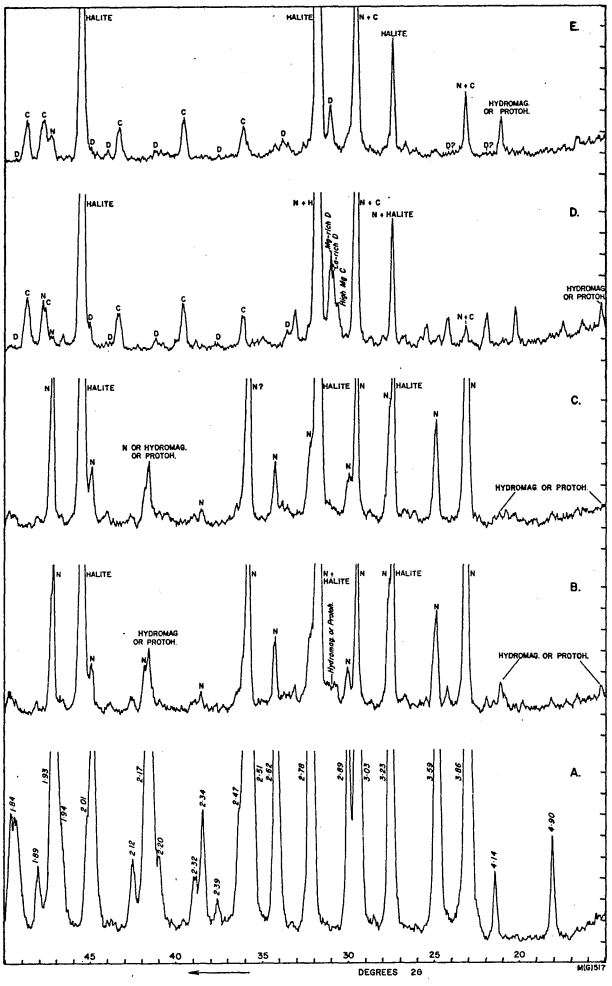
E.
HALITE
HALITE
N + C
HALITE
N + C
HYDROMAG. OR PROTOH.
D.
HALITE
N + H
N + C
N + HALITE
Myrich D
Garnich D
High Mg C
HYDROMAG OR PROTOH.
C.
HALITE
N OR HYDROMAG. OR PROTOH.
HALITE
HALITE
HYDROMAG OR PROTOH.
B.
HALITE
HYDROMAG OR PROTOH.
N + HALITE
Hydromag or Protoh.
HALITE
HYDROMAG. OR PROTOH.
A.
1.84
1.89
1.93
1.94
2.01
2.12
2.17
2.20
2.32
2.34
2.39
2.47
2.57
2.62
2.78
2.89
3.03
3.13
3.32
3.86
4.14
4.90
45
40
35
30
25
20
DEGREES 2θ
MIGI517

FIG 12 The variation of Eh and organic carbon in the nesquehonite (B) calcite (C) and dolomite (D) layers.

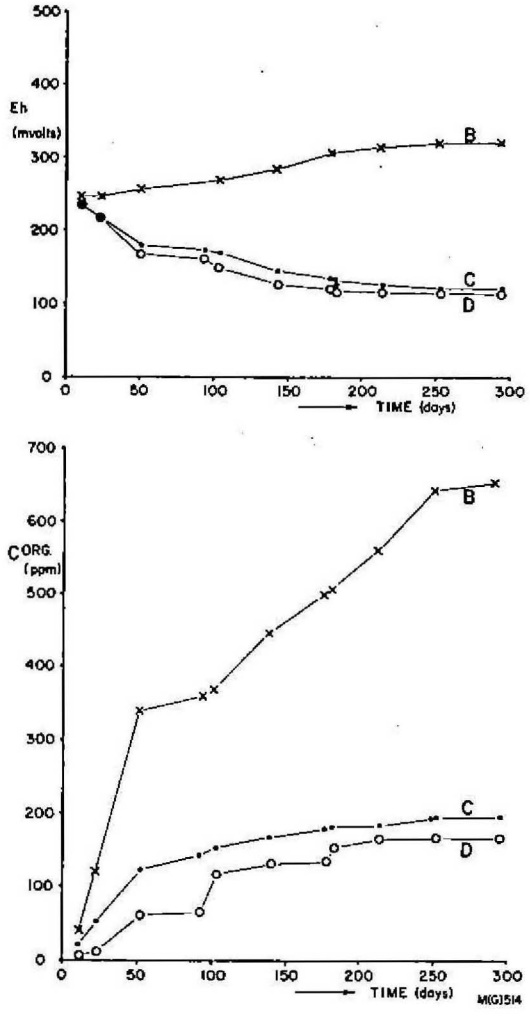
Eh
(mvolts)
500
400
300
200
100
0
B
C
D
0
50
100
150
200
250
300
TIME (days)
C ORG.
(ppm)
700
600
500
400
300
200
100
0
B
C
D
0
50
100
150
200
250
300
TIME (days)
M(G)514

FIG. 13 X-ray diffractograms of dolomite layer taken before (A) and 146 days after (B) the start of the experiment.

D = dolomite

Q = quartz

F = fluorite

C = calcite

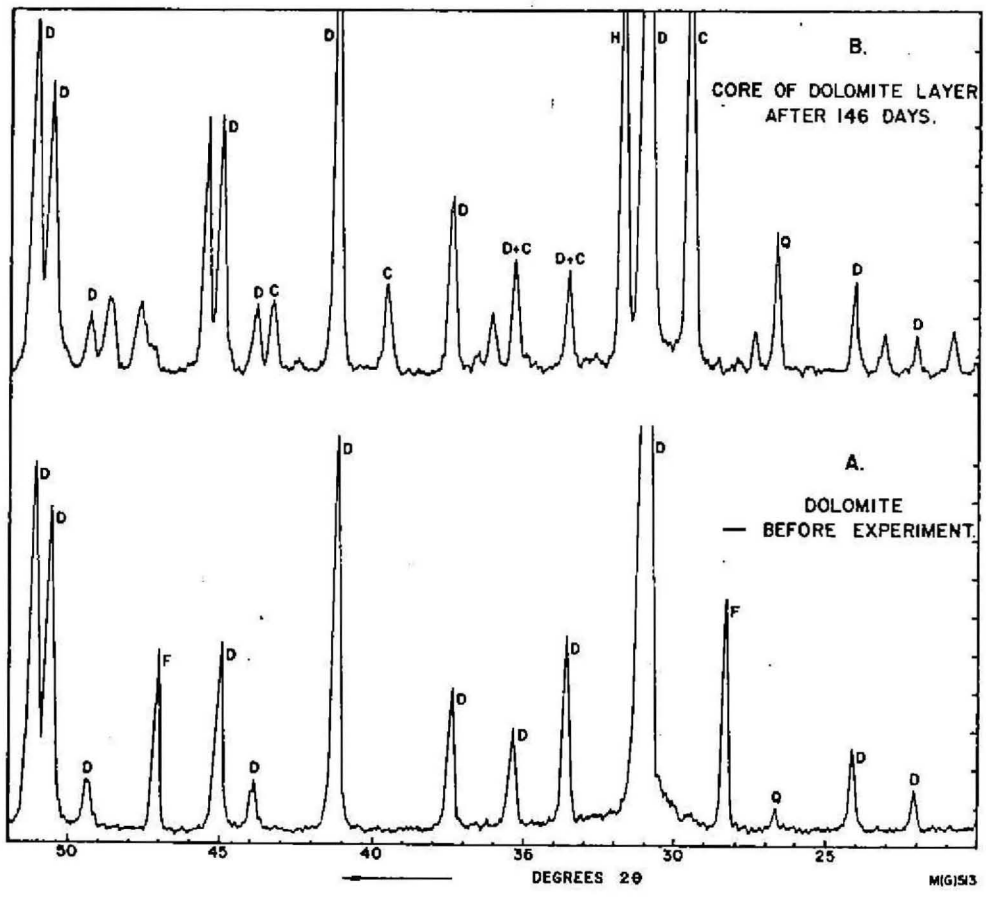
B.
CORE OF DOLOMITE LAYER
AFTER 146 DAYS.
A.
DOLOMITE
— BEFORE EXPERIMENT.
50
45
40
35
30
25
DEGREES 2Θ
M(G)513

FIG. 14. Plot of pH calcite against pH nesquehonite shows an inter-dependent relation over most of the range plotted.

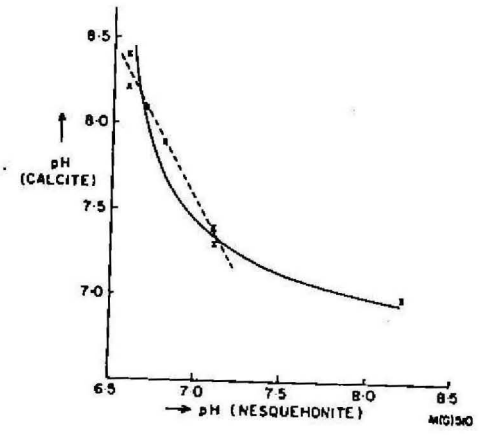
8·5
8·0
7·5
7·0
pH
(CALCITE)
6·5
7·0
7·5
8·0
8·5
pH (NESQUEHONITE)
MG1540

TABLE 1. Periodicity of sampling

TABLE 1

Periodicity of sampling

Parameter	Time (Days) 0	50	100	150	200	250	300
Cores	S S		S	S			S
pH	S S S	S	S S	S	S	S	S
Eh	S S	S	S S	S	S S S	S	S
ORG C.	S S	S	S S	S	S S	S	S
Ca	S				S		
Mg	S				S		
Sr	S				S		
Na	S				S		S
Cl	S				S		S
HCO_3	S		S		S		S

TABLE 2 Changes in the pH and major constituents of the Port Alma and supernatant brines

TABLE 2

Changes in the pH and major constituents of the Port Alma and supernatant brines

	pH	Ca ppm	Mg ppm	Sr ppm	Na%	Cl%	HCO_3^- m eq	Mg/Ca (m)
Port Alma brine	6.95	900	10,020	42	7.70	14.34	150	18.4
Supernatant brine (3 months)	8.1	n.d.	n.d.	n.d.	n.d.	n.d.	1500	
(7.5 months)	7.7	320	12,200	32	8.93	16.76	1600	63
In solution only		284	12,100	27				

Na Supernatant brine/Na - Port Alma brine = 1.16

Cl Supernatant brine/Cl - Port Alma brine = 1.17

Concentration factor calculated from volume changes = 1.21

Concentrations expected from experimental concentration factor of 1.165

Ca = 1050 ppm

Mg = 11,673 ppm

Sr = 49 ppm

TABLE 3 pH, Eh and organic carbon data for the supernatant, nesquehonite, calcite and dolomite layers. The initial pH of the Port Alma brine was 6.95

TABLE 3

pH, Eh and organic carbon data for the supernatant, nesquehonite, calcite and dolomite layers. The initial pH of the Port Alma brine was 6.95

	A = SUPER-NATANT LIQUID		B = NESQUEHONITE LAYER			C = CALCITE LAYER			D = DOLOMITE LAYER		
Date	pH	C^{ORG}_{ppm}	pH	Eh	C^{ORG}_{ppm}	pH	Eh	C^{ORG}_{ppm}	pH	Eh	C^{ORG}_{ppm}
21.11.72	7.5	280	8.0	+250	40	8.2	+240	20	7.5	+240	5
01.12.72	7.6	310	8.0	+250	120	8.2	+220	50	7.4	+220	10
02.01.73	7.7	525	7.9	+260	340	7.4	+180	125	7.2	+170	60
13.02.73	7.9	540	8.0	+267	360	7.2	+175	140	7.2	+165	65
22.02.73	8.1	625	8.1	+270	370	7.0	+170	150	7.3	+150	115
30.03.73	8.2	640	8.2	+285	450	7.0	+145	165	7.4	+125	130
08.05.73	7.9	650	7.2	+305	500	7.3	+135	175	7.8	+120	130
10.05.73	7.9	652	7.2	+315	505	7.4	+135	175	7.5	+115	150
12.06.73	7.8	670	6.8	+315	560	7.9	+125	180	7.7	+115	160
20.07.73	7.7	700	6.7	+320	640	8.1	+120	190	8.0	+116	160
30.08.73	7.7	710	6.6	+320	650	8.2	+120	190	8.2	+119	160

TABLE 4 - Chemical composition and mineralogy of particulate matter fractionated from the supernatant brine 7.5 months after establishment of the sedimentary system. Results are in %, calculated to a salt free basis.

1. Based on analytical and X.R.D. data. Halite was detected in all fractions.

TABLE 4

Chemical composition and mineralogy of particulate matter fractionated from the supernatant brine after 7.5 months

Separation	Centrifugation speed	Mineralogy[1]	Ca%	Sr%	Mg%	ORG% Carbon
			(calculated to a salt-free basis)			
1	100 x G	Aragonite 1.83 Mg-calcites, Ca-Mg-carbonates	25.5		5.02	1.6
2	500 x G	Aragonite 1.81 Mg-calcite Ca-Mg-carbonates	27.5		6.14	5.3
3	3000 x G	Aragonite (?) Mg-calcites Ca-Mg-carbonates	9.14	0.27	10.01	5.1
4	14,400 x G	Halite	1.81	0.05	5.47	10.3
5	100,000 x G	No X.R.D. traces	0.2	0.12	0.2	10.8

1. Based on analytical and X.R.D. data. Halite was detected in all fractions.

TABLE 5 - Comparison of Chemical Data from recent Dolomite Forming Environments with that in the Tank Experiment.

1. Data from Von der Borch (1965)
2. Data from Taylor (In press)
3. Data from Deffeyes et al (1965)
4. Data from Illing et al (1965) & Kinsman (1965)

TABLE 5

Comparison of chemical data from recent dolomite-forming environments with the tank equipment

Parameter	COORONG				Bonaire[3]	Persian Gulf[4]	Tank Experiment
	Dolomite Lake[1]	Dolomite) Magnetite) Lake[2]	Disord. Dolom. Lake[1]	Lake Fell-mongery[2] Feb.& Nov. figures			
Salinity ‰	25-90	25-100	25-90	25-18	35-236	210-257	250
X S.S.W.	0.7-2.5	0.7-2.8	0.7-2.5	0.7-0.5	2-6.8	up to 8	7
Mg/Ca	5-13	9.3-73 (Mainly 9.3-25.6)	2.75-6.1	21-10	5-50	5.20	18-63
Mg ppm	750-2790	598-2500	825-2880	1660-940	1401-9647	1300-5760	10,000-12,000
Ca ppm	104-390	21-450	352-1000	80-94	352-1120	50-3200	900-300
HCO_3 ppm	?	?	?	680-564	121-192	?	150-1500
pH	8.4-7.9	7.9-7.95	8.3-8.9	8.6-8.83	?	6-7.2	6.9-8.2
Temp °C						up to 60°C	10-28°C

1. Von der Borch (1965)
2. Taylor (in press)
3. Deffeyes et al. (1965)
4. Illing et al. (1965); Kinsman (1965)